

1 **Monitoring of microalgal cultivations with on-line, flow-through microscopy**

2

3 Ivo Havlik^{*1}, Kenneth F. Reardon², Mehmet Ünal¹, Patrick Lindner¹, Andreas Prediger¹,

4 Alexander Babitzky¹, Sascha Beutel¹, and Thomas Scheper¹

5

6 ¹ Leibniz University Hannover, Institute of Technical Chemistry, Callinstrasse 5, 30167

7 Hannover, Germany

8 ² Department of Chemical and Biological Engineering, Colorado State University, Fort

9 Collins, CO 80523-1370, USA

10

11

12 *Corresponding author: Ivo Havlik

13 Phone: +49-511-762-2569

14 Email: Havlik@iftc.uni-hannover.de

15

16

17 **Abstract**

18 Microalgal cultivations present challenges for monitoring and process control posed by their
19 large scale and the likelihood that they will be composed of multiple species. Cell
20 concentration is a fundamental parameter in any cultivation but is typically performed using
21 off-line methods that may be time-consuming, laborious, or subject to interferences. Here, an
22 in-situ microscope has been adapted to monitoring microalgal cultivations by adding a flow-
23 through cell and adjusting image-processing algorithms. After installation in the bypass of a
24 photobioreactor, the microscope enabled the continuous, automated acquisition of cell
25 count, cell size, and cell morphology data on-line during cultivation processes over a period
26 of 20 days, without sampling. The flow-through microscope was tested in cultivations of
27 *Chlamydomonas reinhardtii* and *Chlorella vulgaris*. Cell concentration measurements were in
28 agreement with off-line optical density measurements for both species. In addition, cell size
29 and morphology distributions were obtained that revealed population shifts during the
30 cultivation of *C. vulgaris*. This monitoring system thus provides a means to obtain detailed,
31 non-invasive insights of microalgal cultivation processes.

32

33

34 **Keywords**

35 Flow-through microscopy, microalgae, automated image processing, cell count, cell size
36 distribution

37

38 **1. Introduction**

39 The industrial cultivation of microalgae has been the focus of increased attention in recent
40 years, although the first commercial operations date to the 1960s. Various microalgae are
41 cultivated to produce food, food supplements, pigments, and lipids for conversion to biofuels.
42 Microalgae are usually cultivated in batch or semi-batch processes with cultivation times of
43 up to 20 days. The monitoring of microalgal cultivations is of importance for process control.
44 Of particular interest are parameters related to the biological system, including cell
45 concentration and composition, which provide information about the status of the cultivation.
46 Data on cell morphology and size are useful for monitoring the presence of contaminating
47 species and the health of the culture. Ideally, these measurements would be made
48 continuously, with the sensor system interfaced with the photobioreactor or pond in either an
49 in-situ or an on-line format [1].

50

51 One approach to this goal is the use of continuous, non-invasive microscopic monitoring.
52 The first in-situ microscope (ISM) was developed in 1990 [2] and has since been improved
53 by several researchers [3]. It has been employed for the in-situ monitoring of yeast,
54 mammalian, and microcarrier cultivations as well as crystallization processes of amino acids,
55 proteins, and pharmaceuticals [4]. Most ISM systems are based on a transmitted light
56 microscope and can be mounted in a 25-mm side port of a bioreactor. The sampling zone is
57 thus immersed in the cultivation medium. Images of microorganisms or crystals are acquired
58 and processed using particle-specific algorithms, yielding estimates of several parameters,
59 including particle count, size and morphology.

60

61 The goal of this project was to develop and evaluate the ISM strategy for monitoring
62 microalgal cultivations. Cultivations of two algal species were conducted and compared with
63 standard off-line measurements of optical density.

64

65

66 **2. Materials and Methods**

67 **2.1. Flow-through microscope hardware**

68 The flow-through microscope (FTM) is a modified version of the in-situ microscope ISM III
69 XTF (Sartorius Stedim Biotech GmbH, Göttingen, Germany) [5]. It has been used
70 successfully for monitoring of various biotechnological processes such as cultivations of
71 microorganisms and protein crystallization. The ISM III XTF is a transmitted light, bright-field
72 microscope that can be mounted in a 25-mm side port of a bioreactor.

73

74 For the monitoring of microalgal cultivations, several modifications of the ISM III XTF were
75 necessary to allow removal of adhered cells within the measuring zone, provide a
76 replaceable light source, and integrate the device into the glass tubular photobioreactor used
77 in this study. To accomplish these goals, the outer tube of the ISM was redesigned by
78 replacing the sampling zone with a flow cell and by adding inlet and outlet metal tubes that
79 can be integrated into the bypass of a photobioreactor. The upper segment of the
80 microscope containing camera, objective lens, and motors was mounted on the outer tube
81 (Fig. 1). Since the whole system has a modular construction, individual parts could be
82 replaced easily. A white LED was attached on the other side of the flow cell (Fig. 1). This
83 construction allowed the flushing of the microscope windows by temporarily increasing the
84 flow rate through the flow cell.

85

86 **2.2. Image analysis and hardware control software**

87 It was also necessary to alter the image-processing algorithms of the ISM III XTF to
88 recognize microalgal cells. The original instrument software includes the control program
89 InSitu Control for controlling the ISM hardware and camera parameters and for recording
90 microscope images, as well as the image processing software InSitu Analysis for performing
91 cell recognition and to allow parameter computation either on- or off-line. The algorithms for
92 image processing for cell detection were originally designed for yeast cells and were based
93 on border-tracking methods. Differences of grey values to the mode value (image

94 background) were used to define the border of possible cell objects. Since algae images
95 tended to be noisier, and consequently produced blurry object borders, this led to processing
96 artifacts in this application to algal cells.

97

98 Modification of the software consisted of migration from Delphi to C#, and implementing the
99 SUSAN procedure [6] for border tracking and cell detection to allow better object recognition
100 from noisy and out-of-focus images. Furthermore, the "Cell Wiper" function was introduced
101 to enable recognition of cells that have stuck to the sampling zone surface. These adhered
102 cells could be then excluded from counting. For each microalgal strain, additional strain-
103 specific algorithm optimization was necessary to account for different cell shapes.

104

105 The resulting software is capable of computing three process variables as primary
106 information: cell count in an image, and cell size and cell eccentricity for each cell identified
107 in the image. Furthermore, the software produces other information from these primary
108 data: cell volume of individual cells, total cell volume in a given liquid volume (biomass
109 concentration), detection of double cells and cell clusters, and classification into large,
110 medium, and small cells. Processing parameters and all results for each image are recorded
111 in a separate file linked to the image. From these files, all data can be exported, for each cell
112 and each image individually or as a summary, into a .csv file. Cell size distributions can also
113 be exported as a histogram. All variables are visualized in the GUI in real time.

114

115 **2.3. Microscope calibration**

116 For absolute cell area determination, the microscope-camera system was calibrated. A film
117 with a microscale was inserted into the measuring zone and pixels over a distance were
118 counted manually in the image. The area of one pixel was computed from pixel count per
119 micrometer. When the 10X microscope objective was used, a pixel had an area of $0.67 \mu\text{m}^2$,
120 while the 20X objective yielded a conversion of $0.17 \mu\text{m}^2$ per pixel.

121

122 **2.4. Photobioreactor system**

123 Two photobioreactor (PBR) cultivation systems were used for testing the FTM. Both are
124 based on glass tubes of 45-cm length and outside diameter of 8 cm (volume 1.9 L) equipped
125 with two tubing connections and an inner glass tube of 2.4-cm inside diameter placed along
126 the centerline. The light source was an Osram 640 13W Universal White fluorescent lamp
127 that was located in the inner glass tube and provided illumination with average intensity
128 (PAR) of $58 \mu\text{mol s}^{-1} \text{m}^{-2}$ as measured 3 cm from the lamp surface. To accommodate the
129 aeration, cooling, and sensors, two variants of a monitoring/addition vessel (MAV) were
130 employed, both with a working volume of about 0.5 L. The first MAV was a glass vessel
131 equipped with sensor ports in the lid for temperature, pH, and pO_2 , and with a gas inlet and
132 outlet. The second MAV was a steel double-jacketed unit with an inoculation port, a mixer,
133 ports for temperature and pH sensors, and connections for gas inlet and outlet. In each
134 experiment, one of these MAVs was attached to the glass tube by flexible tubing, and a
135 peristaltic pump was used to circulate the growth medium between the glass tube and the
136 MAV. Gas sparging took place only in the MAV. The first system, PBR-1, consisted of two
137 glass tubes with the glass MAV and had a total volume of 4.4 L, while PBR-2 consisted of a
138 single glass tube and the stainless steel MAV; this system had a total volume of 2.4 L. In
139 PBR-1, temperature and pH were measured but not controlled, whereas temperature and pH
140 were controlled by a Sartorius control unit Biostat B in PBR-2. In all experiments, CO_2 was
141 supplied by sparging the liquid in the MAV with a mixture of 3% CO_2 in air at 1 vvm. The
142 FTM was placed in the PBR bypass and supplied with cell suspension using a second
143 peristaltic pump (Fig. 2).

144

145 **2.5. Algal cultures, experimental conditions, and measurements**

146 For all cultivation experiments, axenic cultures under sterile conditions were employed. TAP
147 medium [7] was used for all cultivations. On-line cell measurements using the flow-through
148 microscope were evaluated with the modified InSitu Control and InSitu Analysis software.

149

150 A set of four cultivations of *Chlamydomonas reinhardtii* (strain SAG 33.89, SAG Culture
151 Collection, Göttingen, Germany) was performed in the PBR-1 system at approximately 26 °C
152 and pH 7. *C. reinhardtii* is a green microalga with approximately spherical shape and a
153 diameter of 14 to 22 µm. Cultivations were inoculated with a 100-mL culture of *C. reinhardtii*
154 cells grown for 10 days in an illuminated shake flask. The optical density (OD) during the
155 cultivation experiments was measured off-line at 550 nm approximately every 24 h using a
156 Uvikon spectrophotometer. A 10X objective was used in the flow-through microscope. The
157 on-line cell count was computed as cell count/image. Image acquisition and evaluation was
158 performed in cycles every hour, each cycle comprising 100 images in 1-s interval.

159

160 A second set of two cultivations was carried out using *Chlorella vulgaris*, a green microalga
161 with spherical shape and a diameter of 4 to 10 µm. The cultivation was performed in the
162 PBR-2 system at 26 °C and pH 7, inoculated with a 100-mL culture of *C. vulgaris* cells grown
163 for 10 days in an illuminated shake flask. The optical density was measured at 750 nm,
164 outside the absorption range of both chlorophyll a and chlorophyll b, to avoid interference by
165 variable chlorophyll content. As *Chlorella* cells are smaller, a 20X objective was used in the
166 flow-through microscope. The on-line cell count was measured as in the *C. reinhardtii*
167 cultivation and computed also as cell count/image.

168

169

170 **3. Results and Discussion**

171 **3.1. *C. reinhardtii* cultivation monitoring**

172 For the initial evaluation of the FTM for algal cultivation monitoring, cell number
173 concentrations were computed from the analysis of images acquired by the FTM during the
174 *C. reinhardtii* cultivations. Figure 3 is a comparison of these FTM-derived data with the off-
175 line OD measurements at 550 nm. Although the data computed from the images of the flow-
176 through microscope became noisier after 300 h of cultivation, filtering using a 12-h
177 asymmetric median was successful in providing a smoother output. Another comparison of

178 the on-line FTM data and the off-line OD measurements was the calculation of the ratio of
179 the off-line optical density and the median of the cell count obtained from the flow-through
180 microscope data. Ideally, this ratio should be constant during the cultivation no matter the
181 dimensioning of both variables. In these measurements, the relative difference between the
182 two methods decreased with increasing cell concentration (Supplemental Data Figure S-1).

183

184 **3.2. *C. vulgaris* cultivation monitoring**

185 Based on experiences gained during the analysis of the first set of experiments, the data
186 collected by the FTM during the *C. vulgaris* cultivations were analyzed using several
187 additional methods. To account for the presence of a small number of clusters of cells that
188 might skew the data, information from the cell size and eccentricity data collected by the
189 FTM were used to create a function for elimination of likely cell clusters. FTM images from
190 the early growth phase were manually evaluated to determine the parameters of this
191 function, which is shown in Supplemental Data Figure S-2. Cell clusters were screened as
192 follows: (a) all objects larger than 1400 pixels were assumed to be clusters, (b) all objects
193 smaller than 600 pixels were assumed to be single cells, and (c) for objects in the size range
194 600 – 1400 pixels, objects below the corresponding critical eccentricity for a given pixel size
195 (Supplemental Data Figure S-2) were assumed to be single cells. This screening process
196 resulted in the elimination of 3.6% of the images in the early and late growth phases, and 4%
197 of the images in the stationary phase. These procedures yielded a dataset containing all
198 cells identified in the images acquired during the whole cultivation, with every cell linked to
199 its size and eccentricity, with cell clusters eliminated. All subsequent analyses resulting in
200 cell size and eccentricity distributions were carried out using individual cells and their
201 individual parameters.

202

203 These corrected, individual cell data were used to determine cell number concentrations in
204 1-h cycles, and these 1-h data were smoothed using a 12-h asymmetric moving average
205 filter to compare them to the off-line OD measurements (Fig. 4). As with the *C. reinhardtii*

206 cultivations, the on-line data were in good agreement with the off-line OD measurements,
207 although the FTM values were somewhat lower near the start of the experiment (until about
208 165 h). Three growth phases were delineated: early growth (94–179 h), late growth (180–
209 263 h), and stationary (264–335 h).

210

211 Cell size distributions were computed from the corrected FTM data separately for each of the
212 three growth phases (Figure 5). A substantial shift in the size distribution between the early
213 growth and the later two stages can be observed by comparing average and median cell
214 sizes for each stage, computed from the dataset containing all cells detected in FTM images.
215 Average cell sizes in the early, late and stationary phases were 77, 65 and 65 μm^2 ,
216 respectively, and median cell sizes were 71, 61 and 62 μm^2 , respectively. Specifically, the
217 cell population became smaller on average after the first 180 h because of the loss of larger
218 (90–160 μm^2) cells. Distributions of cell size in bar chart format are shown in Supplemental
219 Data Figure S-3. Using off-line measurements in a Coulter Counter, Work et al. [8]
220 determined that *C. reinhardtii* CC124 cells grown in nitrogen-replete medium (corresponding
221 to the early growth phase) were 13% larger than cells grown in nitrogen-deficient medium
222 (corresponding to late growth and stationary phases). This shift in size distribution could
223 explain the differences between the OD and FTM measurements between 100 and 200 h.

224

225 Similarly, distributions of the cell morphology, expressed as eccentricity, were obtained from
226 the *C. vulgaris* dataset, resulting from the analysis of FTM images corrected for presence of
227 clusters. Distributions of eccentricity data in each of the three cultivation phases are shown
228 in Figure 6, and distributions of eccentricity in bar chart format are shown in Supplemental
229 Data Figure S-4. During the early growth phase, the *C. vulgaris* cells were less elongated
230 than those later in the cultivation.

231

232 **3.3. General aspects of in-situ, flow-through microscopy of microalgal cultivations**

233 Although microalgal cell concentration data can be obtained off-line using flow cytometry,

234 Coulter Counters, and optical absorbance, the results presented here are the first reports of
235 on-line, automated, continuous measurement of microalgal cell concentration. While other
236 methods such as optical absorbance can be modified for on-line application, the need to
237 provide dilution at higher cell concentrations, to avoid wavelengths affected by pigments,
238 and to correct for changes in cell size and composition (e.g., the presence of lipid bodies)
239 has proven challenging. Using FTM, these issues can be avoided, and additional
240 measurements such as the distributions of cell size and cell shape can be obtained.
241 Although shear stress from pumping the cells through the bypass may be a concern for
242 some microalgae, there was no discernible impact for the two species used in these
243 experiments.

244

245 Continuous measurements of cell concentration and cell size distribution have many
246 potential uses in large-scale microalgal cultivations. Nutrient addition and harvesting
247 strategies could be triggered when a particular cell concentration is reached, corrective
248 actions could be taken if the growth rate is not as expected, or the impact of predators (e.g.,
249 rotifers) could be detected at an early and potentially correctable stage. The additional
250 information content of continuous cell size distribution measurements could also provide
251 evidence of lipid accumulation (if associated with cell size increase) and the presence of
252 non-target microbial species. Those goals would be aided by modification of the image-
253 analysis software to provide data on the population morphology.

254

255 The modifications to the commercial ISM described here allow the imaging zone to be
256 cleaned automatically in the event of moderate cell adhesion. If more severe cell
257 accumulation is encountered, the microscope can easily be disconnected, cleaned, and
258 connected again under sterile conditions. Moreover, different light sources can be used with
259 simple replacement.

260

261 The results reported here demonstrate the basic capabilities of this system for obtaining on-
262 line data during algal cultivations. Such a system can enable the collection of a high density
263 of information about cultivations in laboratory and commercial systems, potentially leading to
264 new insights into the basic and applied biology of algae.

265

266

267 **References**

- 268 [1] T. Scheper, B. Hitzmann, E. Stark, R. Ulber, R. Faurie, P. Sosnitza, K.F. Reardon,
269 Bioanalytics: detailed insight into bioprocesses, *Analytica Chimica Acta* 400 (1999) 121-
270 134.
- 271 [2] H. Suhr, P. Speil, G. Wehnert, W. Storhas, *In situ-Mikroskopiesonde und Messverfahren*,
272 Germany, 1990.
- 273 [3] T. Hopfner, A. Bluma, G. Rudolph, P. Lindner, T. Scheper, A review of non-invasive
274 optical-based image analysis systems for continuous bioprocess monitoring, *Bioprocess*
275 *and Biosystems Engineering* 33 (2010) 247-256.
- 276 [4] A. Bluma, T. Hopfner, A. Prediger, A. Glindkamp, S. Beutel, T. Scheper, *Process*
277 *analytical sensors and image-based techniques for single-use bioreactors*, *Engineering*
278 *in Life Sciences* 11 (2011) 550-553.
- 279 [5] G. Rudolph, P. Lindner, A. Gierse, A. Bluma, G. Martinez, B. Hitzmann, T. Scheper,
280 *Online monitoring of microcarrier based fibroblast cultivations with in situ microscopy*,
281 *Biotechnology and Bioengineering* 99 (2008) 136-145.
- 282 [6] S.M. Smith, J.M. Brady, *SUSAN - A new approach to low level image processing*,
283 *International Journal of Computer Vision* 23 (1997) 45-78.
- 284 [7] E.H. Harris, *The Chlamydomonas Sourcebook: Introduction to Chlamydomonas and Its*
285 *Laboratory Use*, 2nd Edition, Academic Press, 2008.
- 286 [8] V.H. Work, R. Radakovits, R.E. Jinkerson, J.E. Meuser, L.G. Elliott, D.J. Vinyard, L.M.L.
287 Laurens, G.C. Dismukes, M.C. Posewitz, *Increased Lipid Accumulation in the*

288 *Chlamydomonas reinhardtii* sta7-10 Starchless Isoamylase Mutant and Increased
289 Carbohydrate Synthesis in Complemented Strains, Eukaryotic Cell 9 (2010) 1251-1261.
290
291
292

293 **Figure captions**

294

295 Figure 1. Schematic of the flow-through microscope. Inset: detail of measuring zone.

296

297 Figure 2. Schematic of the flow-through microscope placement in the photobioreactor
298 bypass.

299

300 Figure 3. Comparison of off-line cell density measurements (OD) with data computed from
301 in-situ FTM analysis during a cultivation of *Chlamydomonas reinhardtii*. Raw data were
302 smoothed with a 12-h asymmetric median filter.

303

304 Figure 4. Comparison of off-line cell density measurements (OD_{750}) with data computed
305 from in-situ FTM analysis during a cultivation of *Chlorella vulgaris*. Cell count data were
306 acquired and computed every hour, and were smoothed by a 12 h asymmetric moving
307 average filter.

308

309 Figure 5. Cell size distributions in different phases of a *C. vulgaris* cultivation in PBR-2 as
310 measured by the FTM. Phase 1 is the early growth phase (94-179 h), Phase 2 is the
311 late growth phase (180-263 h), and Phase 3 is the stationary phase (264-335 h). Data
312 resulting from cell clusters were removed using the experimentally derived function
313 described in the text.

314

315 Figure 6. Distributions of *C. vulgaris* morphology in terms of eccentricity during different
316 phases of a *C. vulgaris* cultivation in PBR-2 as measured by the FTM. Eccentricity is
317 defined such that a value of 1.0 corresponds to a circle and larger values are ellipses.
318 Phase 1 is the early growth phase (94-179 h), Phase 2 is the late growth phase (180-
319 263 h), and Phase 3 is the stationary phase (264-335 h). Data resulting from cell
320 clusters were removed using the experimentally derived function described in the text.

1 **Monitoring of microalgal cultivations with on-line, flow-through microscopy**

2

3 Ivo Havlik*¹, Kenneth F. Reardon², Mehmet Ünal¹, Patrick Lindner¹, Andreas Prediger¹,

4 Alexander Babitzky¹, Sascha Beutel¹, and Thomas Scheper¹

5

6

7 **Acknowledgments**

8 This work was supported by the Sustainable Bioenergy Development Center of Colorado

9 State University and by funds from the Jud and Pat Harper Professorship in Chemical and

10 Biological Engineering (to KFR).

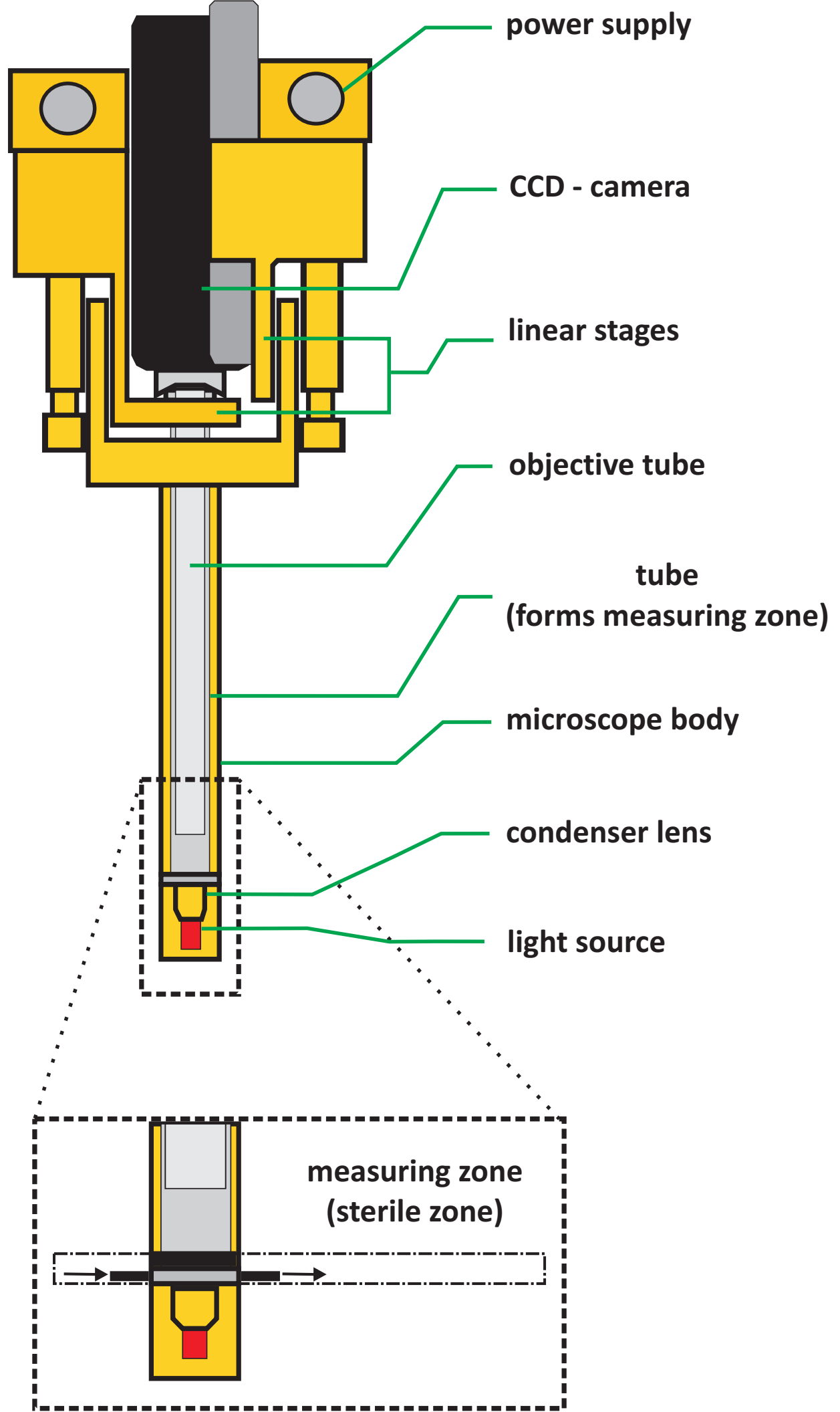
11

12

Figure

upper segment

lower segment



Figure

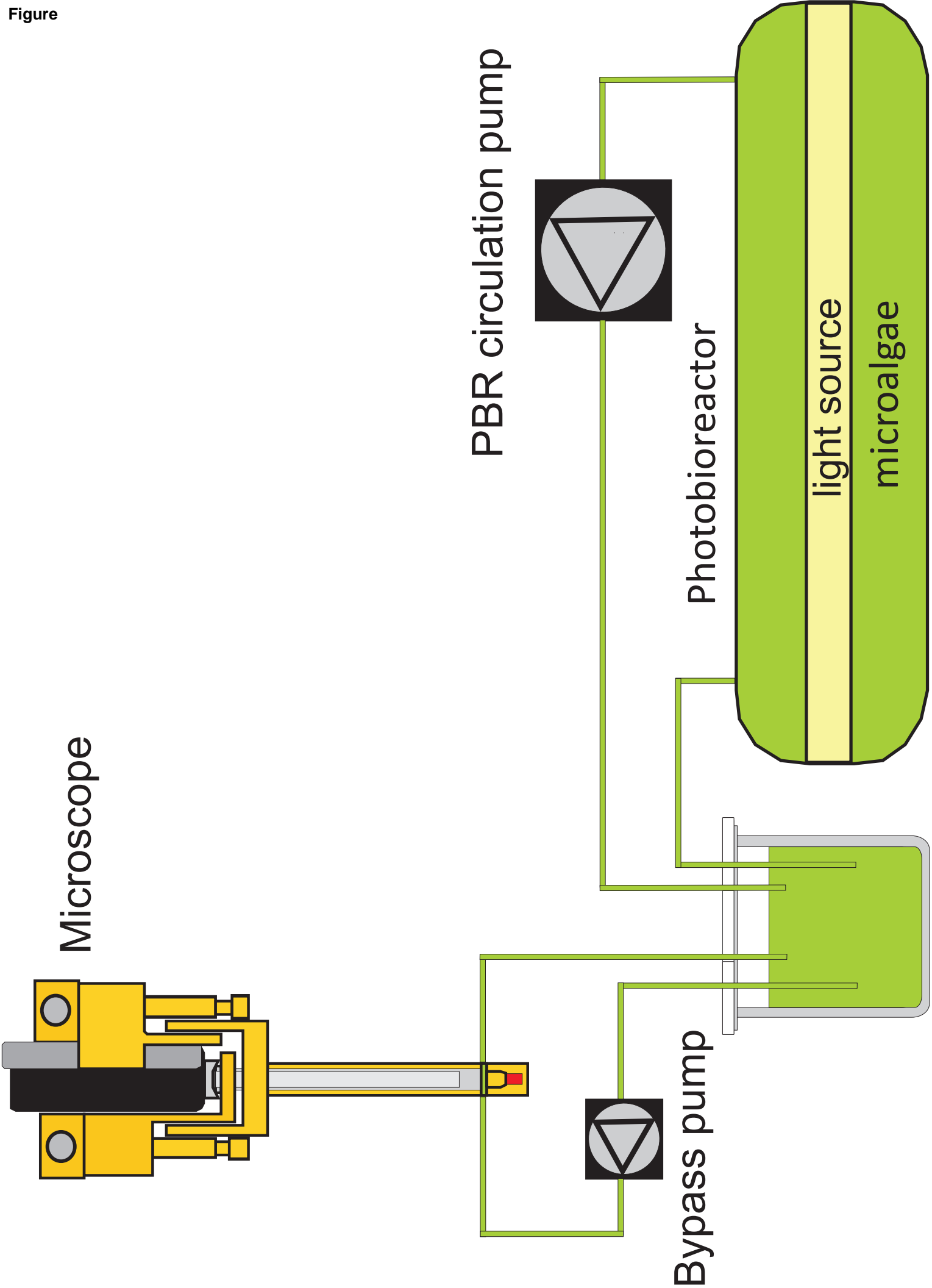


Figure
[Click here to download high resolution image](#)

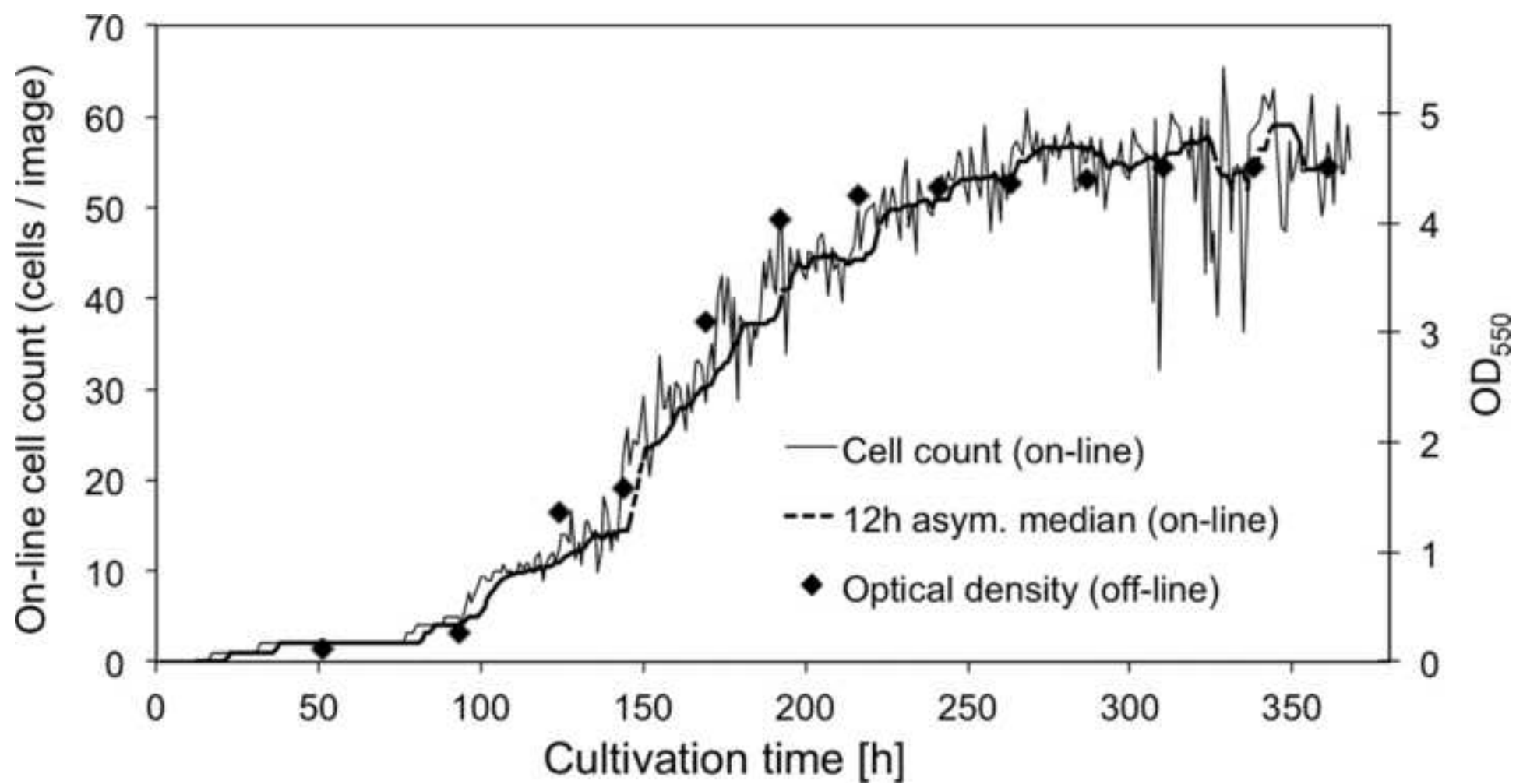


Figure
[Click here to download high resolution image](#)

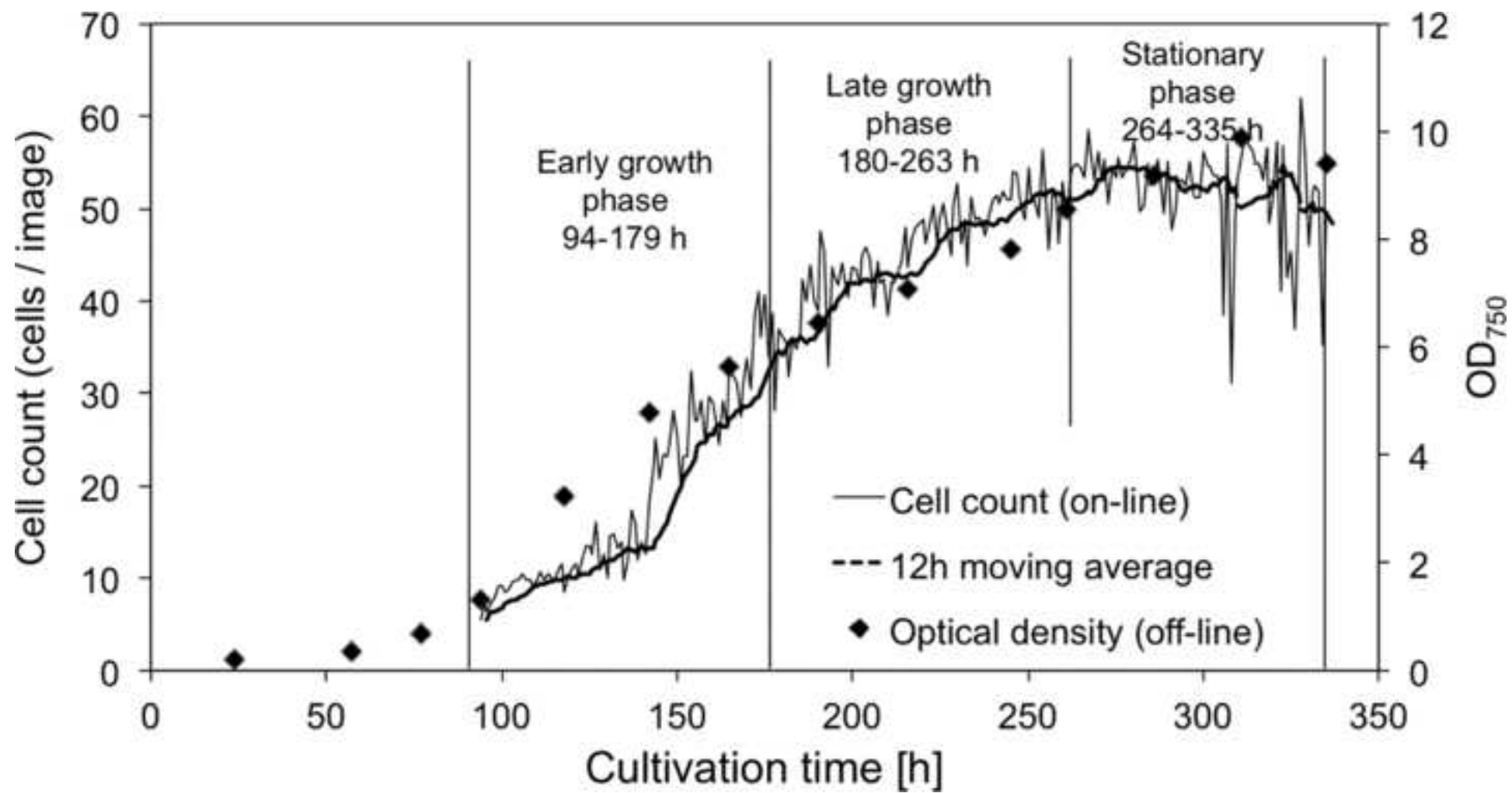


Figure
[Click here to download high resolution image](#)

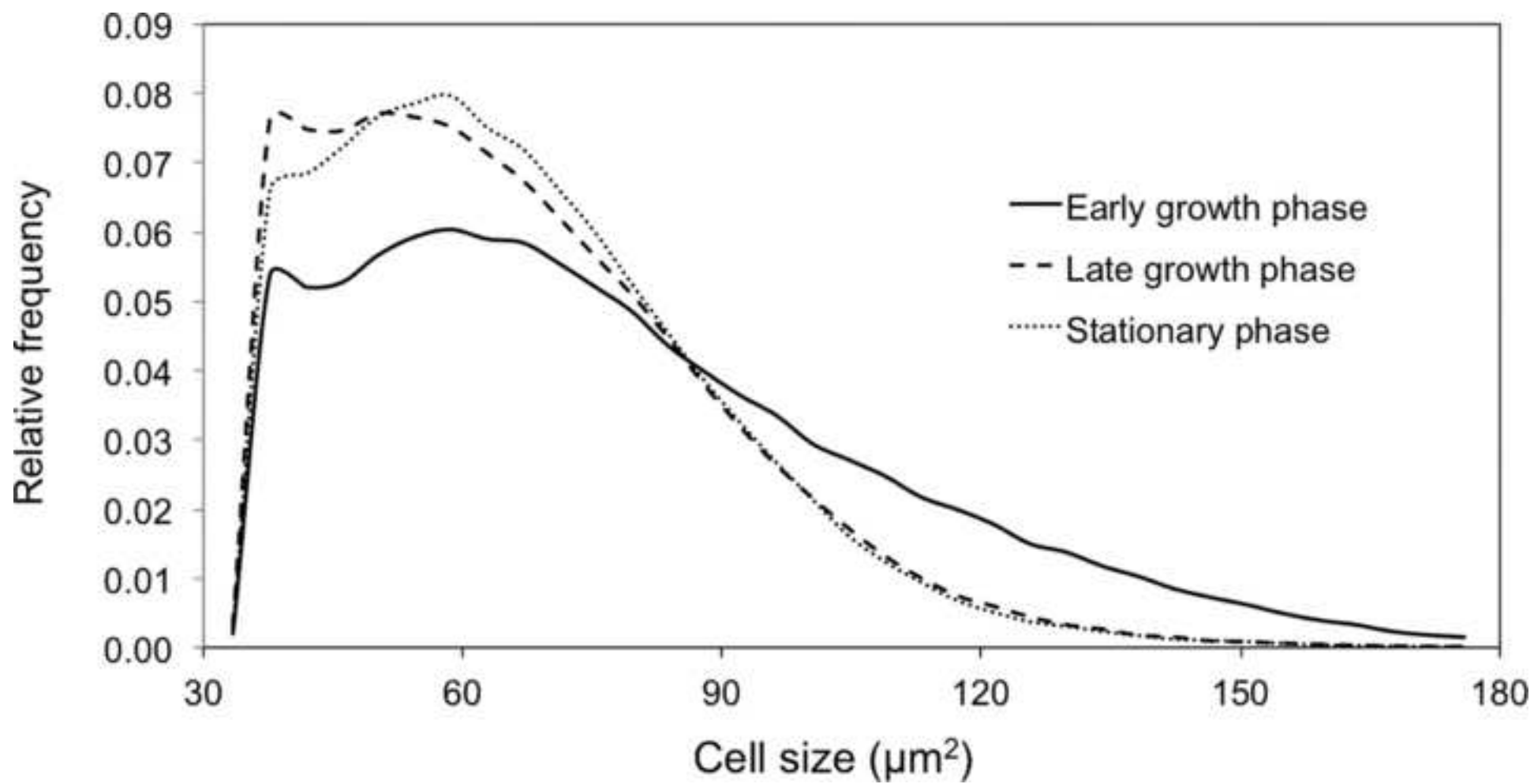
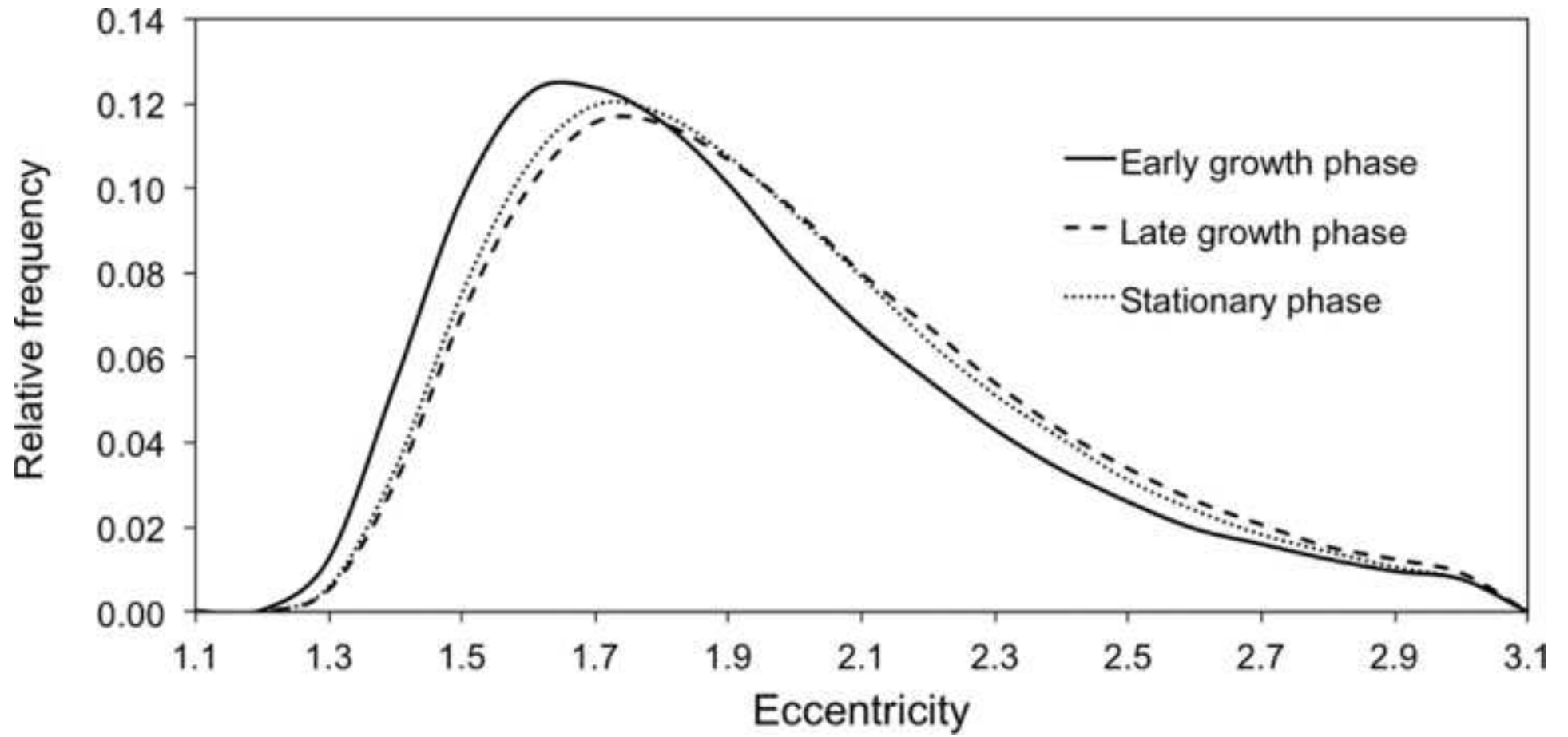


Figure
[Click here to download high resolution image](#)



Supplemental Information for
Monitoring of microalgal cultivations with on-line, flow-through microscopy
Ivo Havlik*, Kenneth F. Reardon, Mehmet Ünal, Patrick Lindner, Andreas Prediger, Alexander Babitzky, Sascha Beutel, and Thomas Scheper

Contents:

Figure S-1. Relative deviations of the ratio of off-line OD to on-line FTM cell counts from the mean of 0.83 computed over an entire cultivation of *Chlamydomonas reinhardtii*.

Figure S-2. Critical eccentricity function for analysis of *Chlorella vulgaris* image data.

Figure S-3. Distributions of cell size during different phases of a *Chlorella vulgaris* cultivation in PBR-2 as measured by the FTM.

Figure S-4. Distributions of morphology in terms of eccentricity during different phases of a *Chlorella vulgaris* cultivation in PBR-2 as measured by the FTM.

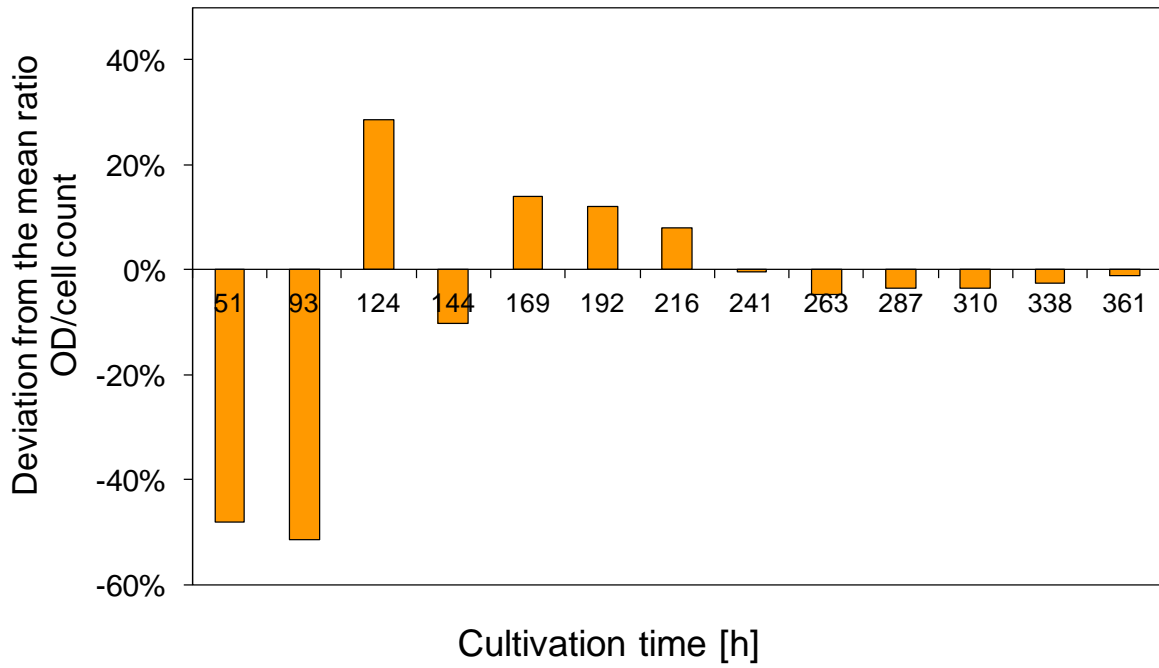


Figure S-1. Relative deviations of the ratio of off-line OD to on-line FTM cell counts from the mean of 0.83 computed over an entire cultivation of *Chlamydomonas reinhardtii*.

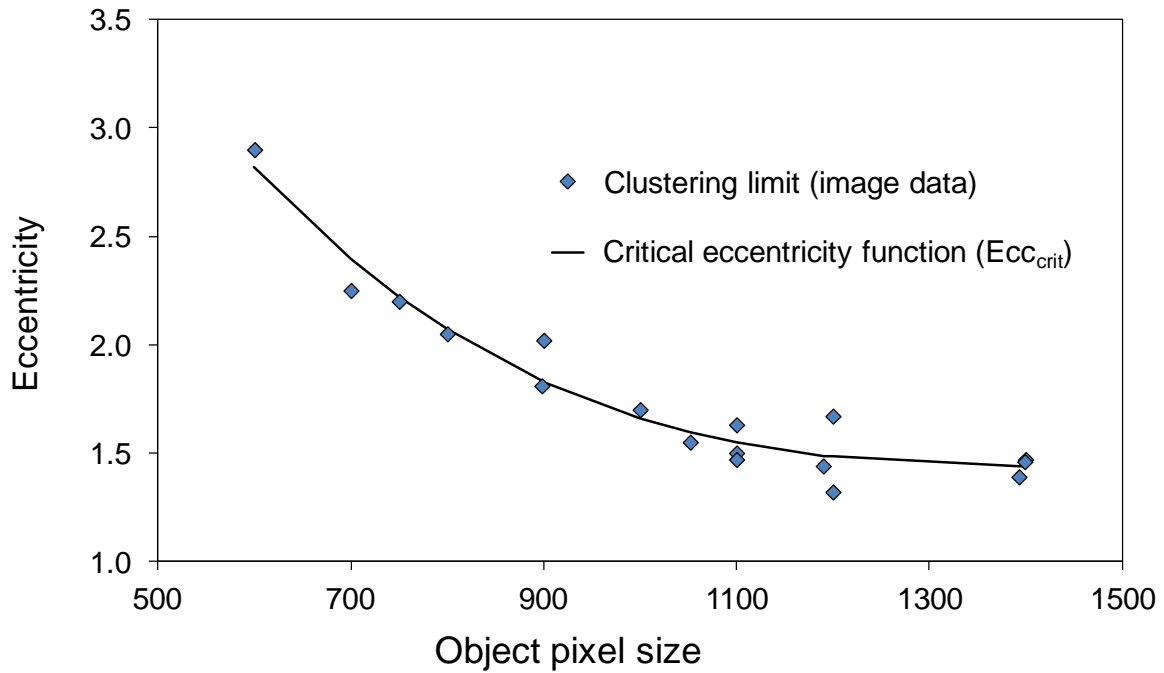


Figure S-2. Critical eccentricity function for analysis of *Chlorella vulgaris* image data. Manually selected image data (only in the early growth phase) was used to develop a critical eccentricity function for the size range 600 – 1400 pixels that serves to distinguish clusters and large single cells. All objects larger than 1400 px are assumed to be clusters, all objects smaller than 600 px are assumed to be single cells, and for objects in the size range 600 – 1400 px, a critical eccentricity is computed. All objects below the critical eccentricity (provided by the function) for a given pixel size are assumed to be single cells. Objects classified as clusters can be then removed from further analysis concerning cell size and eccentricity.

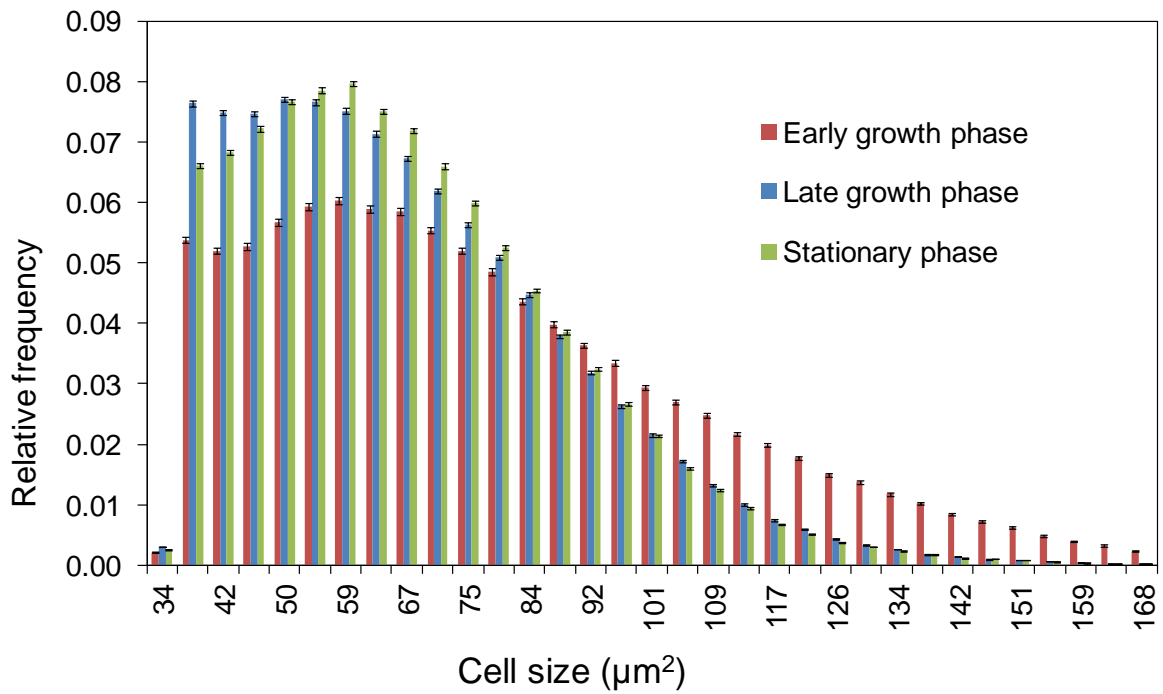


Figure S-3. Distributions of cell size during different phases of a *Chlorella vulgaris* cultivation in PBR-2 as measured by the FTM. The early growth phase (94-179 h), the late growth phase (180-263 h), and the stationary phase (264-335 h) are shown. Data resulting from cell clusters were removed using the experimentally derived function described in the text. Error bars were calculated for individual histogram bins by assuming Poisson distribution of count error; to normalize for relative frequency, the error in each bin with count N is equal to $\pm \sqrt{N} / \sum(N_1 \dots N_{20})$.

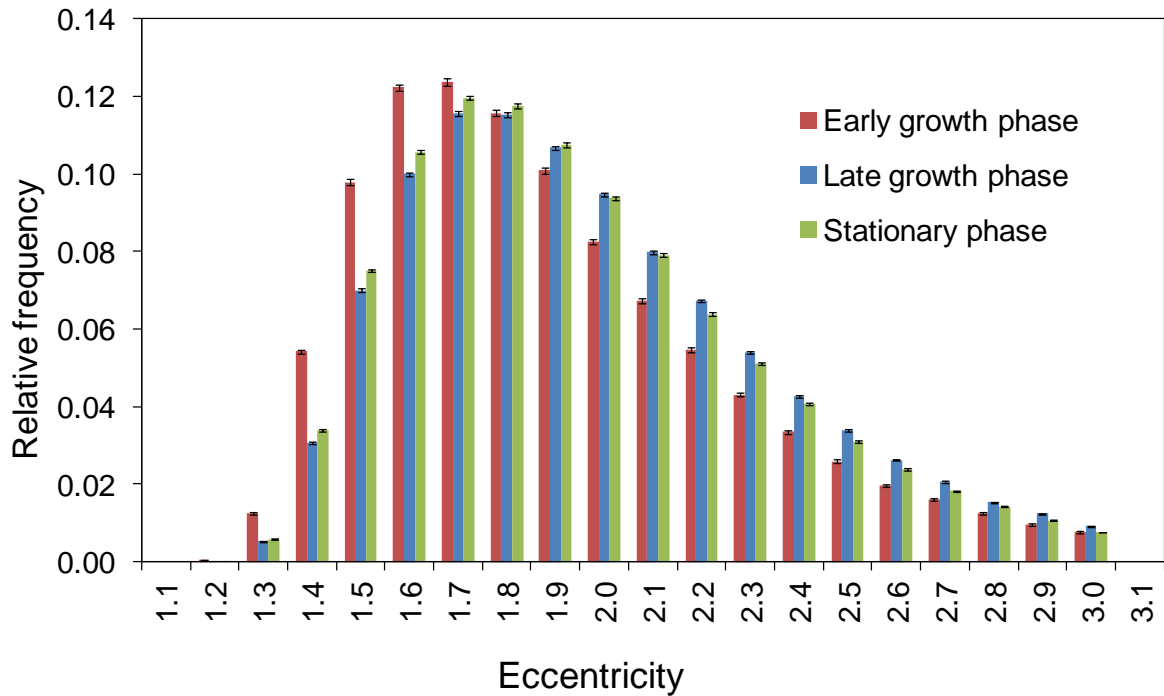


Figure S-4. Distributions of morphology in terms of eccentricity during different phases of a *Chlorella vulgaris* cultivation in PBR-2 as measured by the FTM. Eccentricity is defined such that a value of 1.0 corresponds to a circle and larger values are ellipses. The early growth phase (94-179 h), the late growth phase (180-263 h), and the stationary phase (264-335 h) are shown. Data resulting from cell clusters were removed using the experimentally derived function described in the text. Error bars were calculated for individual histogram bins by assuming Poisson distribution of count error; to normalize for relative frequency, the error in each bin with count N is equal to $\pm \sqrt{N} / \sum(N_1..N_{20})$.